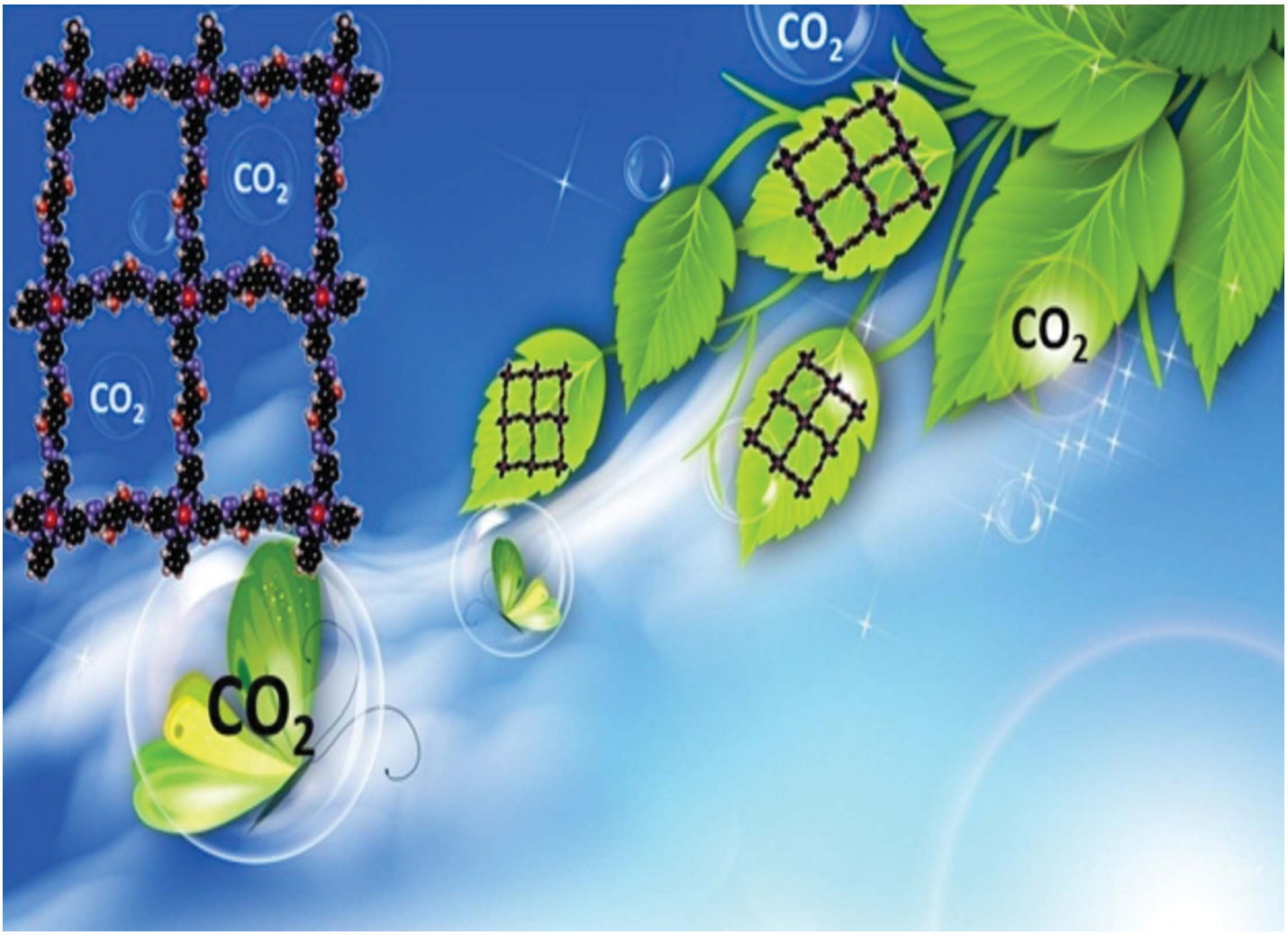

Showcasing studies of CO_2 capture using phthalocyanines-based porous polymers by Prof. Luis Echegoyen's carbon nanomaterials laboratory at the University of Texas at El Paso.

Title: High and selective CO_2 adsorption by a phthalocyanine nanoporous polymer

A rigid macrocyclic phthalocyanine-based porous polymer was synthesized by a one pot "click" reaction between tetraazido-phthalocyanine and bisamine diethynylbenzene; the first example of a phthalocyanine porous polymer used for CO_2 adsorption.

As featured in:

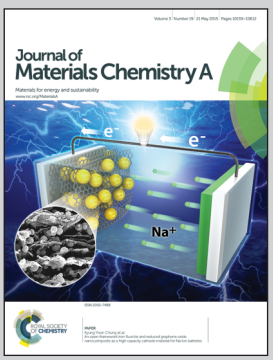

See Luis Echegoyen *et al.*, *J. Mater. Chem. A*, 2015, **3**, 10284.

ROYAL SOCIETY OF CHEMISTRY

www.rsc.org/MaterialsA

Registered charity number: 207890

Journal of Materials Chemistry A

PAPER

View Article Online
View Journal | View Issue

Cite this: J. Mater. Chem. A, 2015, 3, 10284

Received 23rd January 2015
Accepted 19th March 2015

DOI: 10.1039/c5ta00587f

www.rsc.org/MaterialsA

High and selective CO_2 adsorption by a phthalocyanine nanoporous polymer†

Venkata S. Pavan K. Neti,[a] Jun Wang,[b] Shuguang Deng[b] and Luis Echegoyen*[a]

A rigid macrocyclic phthalocyanine-based porous polymer, CPP, was synthesized by a one pot "click" reaction between tetraazido-phthalocyanine and bisamine diethynylbenzene. This CPP is the first example of a phthalocyanine porous polymer used for CO_2 adsorption and it shows very high CO_2 adsorption (15.7 wt% at 273 K/1 bar) and high selectivity for CO_2/N_2 (94) and for CO_2/CH_4 (12.8) at 273 K/1 bar. The CPP exhibited a Brunauer–Emmett–Teller (BET) surface area of 579 m^2 g^{-1} and high thermal stability up to 500 °C, thus showing good potential for CO_2 capture.

1. Introduction

CO_2 capture is one of the important challenges that, when solved, would enable the usage of fossil fuels with lower CO_2 emissions. Highly selective CO_2 adsorption on porous organic polymers (POPs)[1–18] is an effective alternative for CO_2 capture over conventional amine scrubbers. To ensure high CO_2 capture, the building blocks for these porous polymers should include functional groups, such as $-NO_2$, –OH, –COOH, $-SO_3H$, arylamines, and heterocyclic nitrogen atoms to enhance CO_2 affinities through $O{=}C{=}O(\delta^-)$–$H(\delta^+)$–O and $H_2N(\delta^-)$–$C(\delta^+)O_2$ interactions.[19] Porous polymers containing CO_2 binding functionalities have the advantage that they can be easily regenerated without applying heat because no chemisorption is involved.

In the past decade, the Cu(I)-catalyzed "click" reaction between alkynes and azides has been widely used in materials science and biology.[20,21] A few porous polymers were prepared using the "click" reaction in part due to the advantage of high thermal and chemical stabilities of the triazole ring, mild reaction conditions, and the absence of by-products.[22–24] Recently, various porous organic materials such as hypercrosslinked polymers (HCPs), polymers of intrinsic microporosity (PIMs), conjugated microporous polymers (CMPs), porous organic frameworks (POFs), benzimidazole-linked polymers (BILPs), porous polymer networks (PPNs), and covalent organic polymers (COPs) have received significant attention due to their potential applications in gas storage and separations.[1–18] Unlike metal–organic frameworks (MOFs)[25–28] and covalent organic frameworks (COFs),[29–37] POPs are amorphous, but have tunable pore sizes and surface areas similar to those of MOFs and COFs. They can be prepared under easily controllable reaction conditions, are amenable to scale-up preparation, and exhibit high stability towards moisture, much better than the corresponding MOFs and COFs.

To the best of our knowledge, a phthalocyanine-based porous polymer has never been reported using "click" polymerization or any other method, and tested for selective CO_2 adsorption studies. Here we report the synthesis of a partially crystalline phthalocyanine porous polymer, CPP, based on a "click" reaction between a phthalocyanine-tetraazide (**1**) and bisamine diethynylbenzene (**2**), see Scheme 1. We investigated the effect of nitrogen-rich functional groups (amine and triazole) inside the pore surfaces. The data reveal high CO_2 adsorption (15.7 wt%), and also high CO_2/N_2 (94) and CO_2/CH_4 (12.8) selectivities.

2. Experimental methods

All chemicals and solvents were purchased from Sigma-Aldrich, and Alfa-Aesar. Tetraaminophthalocyanine Co(II)[41] and bisamine diethynylbenzene[42] were prepared according to literature procedures. Fourier transform Infrared (FT-IR) spectra were recorded on a Perkin-Elmer Spectrum One infrared spectrometer using an ATR attachment. ^{1}H NMR spectra were obtained on a JOEL-600 MHz NMR spectrometer. ^{13}C cross-polarization magic angle spinning (CP-MAS) NMR spectra for solid samples were recorded on a Bruker AVANCE-300 NMR spectrometer. Powder X-ray diffraction (PXRD) data were recorded on a Bruker DiscoverD8 model diffractometer by depositing powders on a plastic substrate, from $2\theta = 1°$ up to 30° with 0.05° increment. Field-emission scanning electron microscopy (FE-SEM) was performed on a Hitachi S-4800 fitted with an EDAX energy-dispersive spectrometry system by adhering sample on a sampling platform. Matrix-assisted laser desorption ionization time-of-flight mass (MALDI-TOF MS) spectra were recorded on a

[a]Department of Chemistry, University of Texas at El Paso, El Paso, TX 79968, USA. E-mail: echegoyen@utep.edu; Fax: +1-915-747-8807; Tel: +1-915-747-7573

[b]Department of Chemical Engineering, New Mexico State University, Las Cruces, NM 88003, USA

† Electronic supplementary information (ESI) available: Fig. S1–S3. See DOI: 10.1039/c5ta00587f

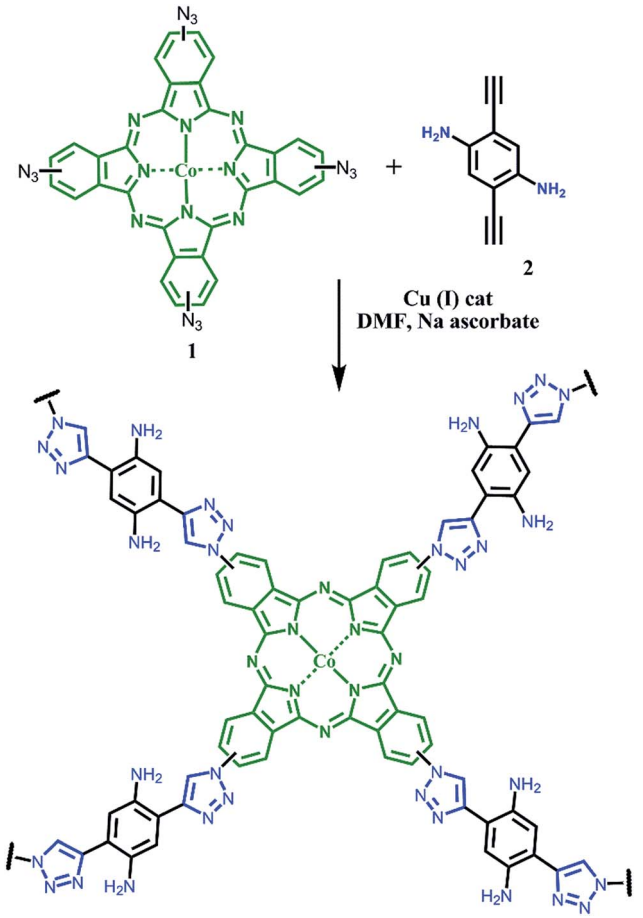

Scheme 1 Synthesis of CPP from tetraazido-phthalocyanine Co(II) and bisamine diethynylbenzene.

Bruker benchtop Microflex model using matrix trihydroxyanthracene. In order to determine pore textural properties including the specific Brunauer–Emmet–Teller (BET) surface area, pore volume and pore size distribution, nitrogen adsorption and desorption isotherms on CPP at 77 K, 273 K, and 298 K were measured on an ASAP-2020 adsorption apparatus (Micromeritics). The samples were degassed *in situ* at 150 °C with a heating rate of 3 °C min^{-1} under vacuum (0.0001 mm Hg) for 12 h before nitrogen adsorption measurements in order to ensure the micro-channels in the structure were guest-free. The Brunauer–Emmett–Teller (BET) method was utilized to calculate the specific surface areas by using the non-local density functional theory (NLDFT) model, and the pore volumes were derived from the sorption curves. Thermogravimetric analyses between 30–800 °C were conducted on a Mettler-Toledo thermogravimetric analyzer under a N_2 atmosphere using a 5 °C min^{-1} ramp time.

Synthesis of tetraazidophthalocyanine Co(II)

Tetraaminophthalocyanine Co(II) (200 mg, 0.3 mmol) was dissolved in a 2 N HCl (10 mL), cooled to 0 °C and a solution of $NaNO_2$ (93 mg, 1.35 mmol) in water (2 mL) was then added drop-wise into the cooled solution. The reaction mixture was kept at 0 °C for 30 minutes before being neutralized with $CaCO_3$. To this mixture was then added a solution of NaN_3 (91 mg, 1.4 mmol) in water (2 mL) at 0 °C. The resulting mixture was allowed to stir at 0 °C for 20 min and then filtered. The collected green solid was washed with water and dried under vacuum to afford tetraazidophthalocyanine Co(II) (150 mg, Yield: 70%).

Synthesis of CPP

Tetraazidophthalocyanine Co(II) (150 mg, 0.2 mmol) was stirred in a 20 mL DMF for 15 min. $CuSO_4 \cdot 5H_2O$ (20 mg, 0.04 mmol), sodium ascorbate (15 mol%) and bisamine diethynylbenzene (62 mg, 0.4 mmol) were added in one pot (see Scheme 1). The mixture was then heated at 100 °C for 24 h to give the corresponding polymer in 89% yield. Elemental analysis (%) calcd $(C_{60}H_{54}N_{30}Co)_n$ C, 58.1; H, 4.3; N, 33.9; found C, 57.23; H, 3.87; N, 34.45, respectively.

3. Results and discussion

The CPP polymer was synthesized using the Cu(I) catalyzed 1,3-dipolar azide–alkyne cycloaddition (CuAAC) reaction (Scheme 1). Triazole linkages were easily formed by condensation of acetylene and azide groups. During the reaction, the color turned from green to colorless, indicating the formation of the phthalocyanine porous polymer. Green powders precipitated, which were collected by filtration. Soxhlet extraction with water, acetone, and dichloromethane were used to remove low-molecular weight by-products and inorganic salts, respectively. The CPP was insoluble in water and common organic solvents such as acetone, hexanes, ethanol, tetrahydrofuran, DMSO, and *N*,*N*′-dimethylformamide.

In order to verify the chemical connectivity and crystallinity of the CPP, Fourier transform infrared spectroscopy (FT-IR), and ^{13}C NMR cross polarization magic angle spinning (CP/MAS), and powder X-ray diffraction analyses were performed. The formation of triazole linkages were confirmed by the FT-IR spectra (Fig. 1A). The absorption peaks for the acetylene bonds at 3281 cm^{-1} disappear, while new stretches are observed at 1615 cm^{-1} for the –N=N– stretch and a weak band at 2923 cm^{-1} for the –C=CH stretch. These confirmed the formation of the triazole bonds. The peak intensity at 2109 cm^{-1} for the azide moieties was highly attenuated. A broad band observed in the 3300–3500 cm^{-1} region was attributed to the presence of primary amine groups in the CPP. The ^{13}C CP/MAS NMR spectrum (Fig. 1B) showed the characteristic peaks at 153 ppm which can be attributed to the carbon atom of the triazole–acetylene linkages. The peaks in the range of 100–150 ppm originate from the carbons of the phthalocyanine units. The results obtained from FT-IR and CP/MAS NMR confirm that the molecular building blocks are linked to each other *via* the formation of triazole linkages.

Powder X-ray diffraction (Cu Kα radiation) was employed to examine the crystallinity of the CPP (Fig. 2). The diffraction pattern displays a low intensity diffraction peak at $2\theta = 9°$, and another low intensity peak at 26°, reflecting the partially

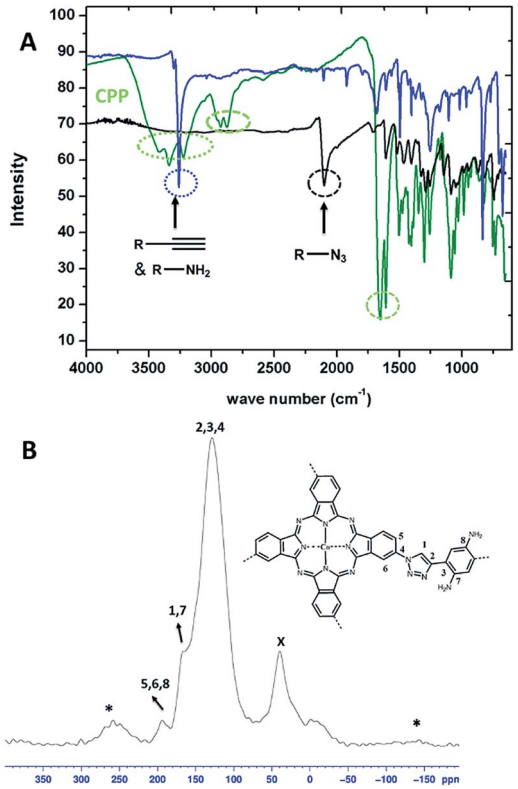

Fig. 1 (A) IR Spectra of **1** (black), **2** (blue) and CPP (green) (B) solid-state ^{13}C CP/MAS NMR spectrum of CPP (X, and "*" represent residual solvent and side bands).

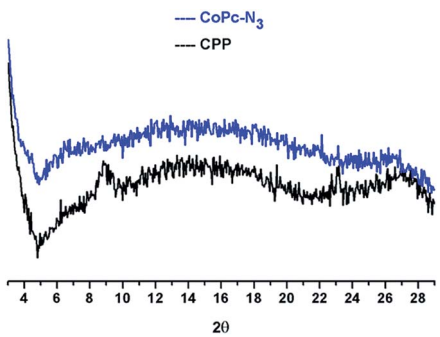

Fig. 2 Powder X-ray diffraction patterns of CoPc-N_3 and CPP.

crystalline nature of CPP. CPP was constructed from a phthalocyanine macrocycle and a small and linear bisamine diethynylbenzene to reduce interpenetration. The porosity parameters of CPP were studied by N_2 adsorption measurements (Fig. 3). The adsorption curves clearly indicated that CPP is microporous and exhibits a type-I reversible adsorption isotherm and the polymer showed selective adsorption towards CO_2 over N_2 and CH_4 (Table 1). The Brunauer–Emmett–Teller (BET) surface area was 579 $m^2\ g^{-1}$ and the total pore volume was 0.71 $cm^3\ g^{-1}$. A relatively small hystereses in the CO_2 uptake data indicates weak interactions between the adsorbent and CO_2 molecules. These weak interactions are crucial for the regeneration of the CPP without applying external energy (heat). The pore size

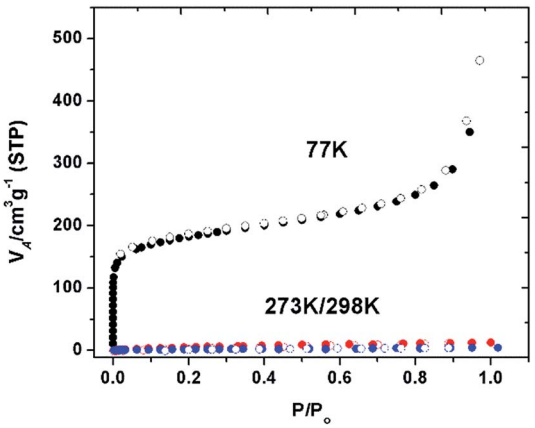

Fig. 3 N_2 at 77 K (black), 273 K (red), and 298 K (blue). Adsorption (filled circles) and desorption (empty circles).

Table 1 Gas adsorption properties of CPP

Polymer	Selectivity	CO_2 (wt%)	CH_4 (wt%)
CPP	94 (CO_2/N_2) 12.8 (CO_2/CH_4)	15.7 (273 K) 10 (298 K)	1.78 (273 K) 0.95 (298 K)

distribution calculated from non-local density functional theory (NLDFT) models clearly show that micropores are present in the polymer (Fig. 4D). Fig. 3 shows a sharp uptake at relatively low pressures, again indicating the presence of micropores. The CPP mainly contains micropores with very low mesopore volume. The micropore surface area, estimated by the *t*-plot method, was 342 $m^2\ g^{-1}$ and the microporosity (V_{micro}/V_{total}, where V_{micro} is the micropore volume and V_{total} is the total pore volume) of CPP was found to be 0.73 at a relative pressure of 0.4, indicating that the majority of the pores are in the microporous domain. Due to the high nitrogen content and surface area of CPP, we assessed the performance of CPP for CO_2 adsorption (Fig. 4A). CO_2 isotherms showed an uptake of 3.57 mmol g^{-1} (15.7 wt%) at 273 K and 2.27 mmol g^{-1} (10 wt%) at 298 K. Although a few phthalocyanine-based polymers of intrinsic microporosity (PIMs) are known, their CO_2 adsorption properties are unknown.[38–40] The CO_2 uptake of CPP at 273 K/1 bar is higher than previously reported for non-phthalocyanine "click" porous polymer networks, such as SNU-C1-sca (13.8 wt% at 273 K/1 bar) and a "click" hyper cross-linked polymer (15.5 wt% at 195 K/1 bar).[23,24] The CO_2 uptake value of CPP exceeds those of primary amine functionalized 2D porous polymers but is lower than the values observed for 3D adamantine based post synthetically modified primary amine porous polymers.[43,44] It should be noted that the CO_2 uptake of amine free CPP, another polymer made with tetraazido-phthalocyanine Co(II) and diethynylbenzene showed 1.8 mmol g^{-1} (8.2 wt%) CO_2 uptake at 273 K/1 bar.

The isosteric heat of adsorption (Q_{st}) of the CPP (33.5 kJ mol^{-1}) was calculated from the CO_2 uptake data at 273 and 298 K by using the van't Hoff equation (Fig. S2†) and the Q_{st} value is below 40 kJ mol^{-1} (chemisorption). Both selectivity and Q_{st} values were calculated following a literature procedure.[12]

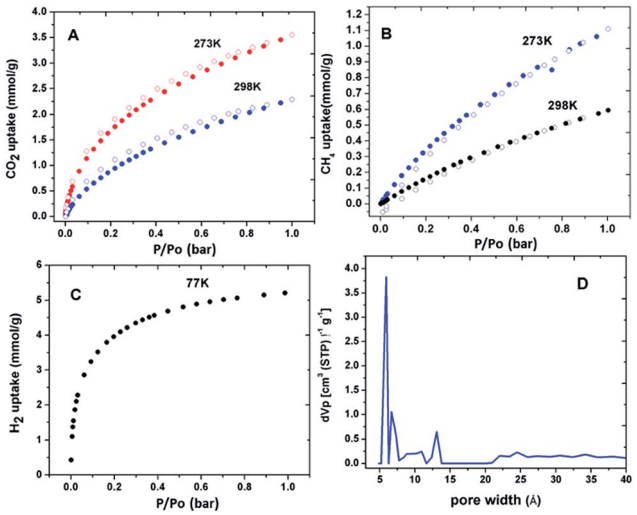

Fig. 4 (A and B) CO_2, and CH_4 at 273 K and 298 K. (C) H_2 at 77 K (D) NLDFT pore size distribution analysis. Adsorption (filled circles) and desorption (empty circles).

Hence, the high CO_2 affinity of the CPP is mainly attributed to the R–N(δ^-)–C(δ^+)O_2 interactions. N_2 and CH_4 adsorption measurements were made under similar conditions to determine the selectivity. On the basis of Langmuir model fits and Henry's constant values in the pressure range between 0 and 1 bar, the estimated adsorption selectivity for CO_2/N_2 is 94 and for CO_2/CH_4 it is 12.8 at 273 K/298 K/1 bar (Fig. S1†). The maximum uptakes are 0.9 wt% for H_2 at 77 K/1 bar and 1.78 wt% for CH_4 at 273 K/1 bar (Fig. 4B and C). Similar results have been reported for POPs, which exhibit lower selectivities than CPP.[13,15,18] At zero coverage, the Q_{st} for CH_4 is 17.2 kJ mol^{-1} (Fig. S2†) which is higher than for other COFs and POPs.[31–34] The CPP showed good thermal stability and was stable at around 500 °C under a N_2 atmosphere, as evidenced by thermogravimetric analysis (Fig. 5).

The field emission scanning electron microscopy (FE-SEM) revealed irregular micron-sized particles (Fig. 6).

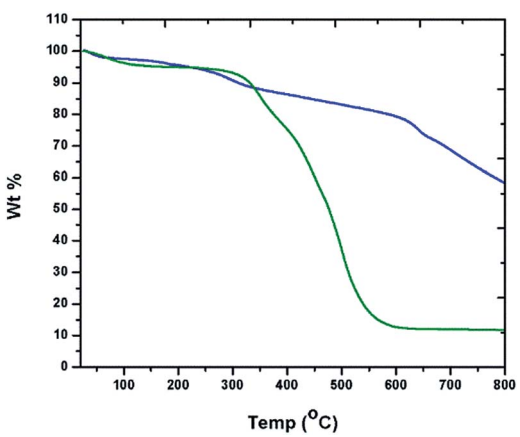

Fig. 5 TGA of CPP (blue) and tetraazido-phthalocyanine Co(II) (green).

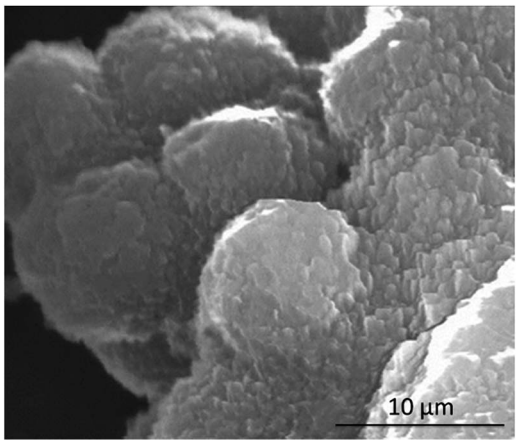

Fig. 6 Scanning electron microscope image of CPP.

In conclusion, we have introduced a "click" chemistry-based strategy to synthesize a partially crystalline and highly porous phthalocyanine polymer. The CO_2 uptake of this polymer is higher than for all previously reported "click" polymers. Due to the simplicity of the synthesis and purification and the high gas uptake capacities, CPP shows great promise for CO_2 capture and for other gas storage applications.

Acknowledgements

This work was generously supported by NSF grant DMR-1205302 (PREM program), and the Robert A. Welch Foundation, grant # AH-0033.

References

1 N. B. McKeown and P. M. Budd, *Chem. Soc. Rev.*, 2006, **35**, 675.
2 M. P. Tsyurupa and V. A. Davankov, *React. Funct. Polym.*, 2006, **66**, 768.
3 J.-X. Jiang, F. Su, H. Niu, C. D. Wood, N. L. Campbell, Y. Z. Khimyak and A. I. Cooper, *Chem. Commun.*, 2008, 486.
4 O. K. Farha, Y.-S. Bae, B. G. Hauser, A. M. Spokoyny, R. Q. Snurr, C. A. Mirkin and J. T. Hupp, *Chem. Commun.*, 2010, **46**, 1056.
5 P. Pandey, A. P. Katsoulidis, I. Eryazici, Y. Wu, M. G. Kanatzidis and S. T. Nguyen, *Chem. Mater.*, 2010, **22**, 4974.
6 W. Lu, D. Yuan, D. Zhao, C. I. Schilling, O. Plietzsch, T. Muller, S. Bräse, J. Guenther, J. Blümel, R. Krishna, Z. Li and H.-C. Zhou, *Chem. Mater.*, 2010, **22**, 5964.
7 M. G. Rabbani and H. M. El-Kaderi, *Chem. Mater.*, 2011, **23**, 1650.
8 Y.-Q. Shi, J. Zhu, X.-Q. Liu, J.-C. Geng and L.-B. Sun, *ACS Appl. Mater. Interfaces*, 2014, **6**, 20340.
9 R. Dawson, A. I. Cooper and D. J. Adams, *Prog. Polym. Sci.*, 2012, **37**, 530.
10 Z. Xiang, X. Zhou, C. Zhou, S. Zhong, X. He, C. Qin and D. Cao, *J. Mater. Chem.*, 2012, **22**, 22663.

11 Y. Xu, S. Jin, H. Xu, A. Nagai and D. Jiang, *Chem. Soc. Rev.*, 2013, **42**, 8012.
12 H. A. Patel, S. H. Je, J. Park, D. P. Chen, Y. Jung, C. T. Yavuz and A. Coskun, *Nat. Commun.*, 2013, **4**, 1357.
13 V. S. P. K. Neti, X. Wu, S. Deng and L. Echegoyen, *Polym. Chem.*, 2013, **4**, 4566.
14 J. Wang, J. Huang, X. Wu, B. Yuan, Y. Sun, Z. Zeng and S. Deng, *Chem. Eng. J.*, 2014, **256**, 390.
15 V. S. P. K. Neti, X. Wu, S. Deng and L. Echegoyen, *RSC Adv.*, 2014, **4**, 9669.
16 W. Zhang, P. Jiang, Y. Wang, J. Zhang and P. Zhang, *Catal. Sci. Technol.*, 2015, **5**, 101.
17 H. Cai, F. Bao, J. Gao, T. Chen, S. Wang and R. Ma, *Environ. Technol.*, 2014, 1–8.
18 V. S. P. K. Neti, J. Wang, S. Deng and L. Echegoyen, *RSC Adv.*, 2015, **5**, 10960.
19 S. Yang, J. Sun, A. J. Ramirez-Cuesta, S. K. Callear, W. I. F. David, D. P. Anderson, R. Newby, A. J. Blake, J. E. Parker, C. C. Tang and M. Schröder, *Nat. Chem.*, 2012, **4**, 887.
20 H. C. Kolb, M. G. Finn and K. B. Sharpless, *Angew. Chem., Int. Ed.*, 2001, **40**, 2004.
21 A. Qin, J. Lam and B. Tang, *Chem. Soc. Rev.*, 2010, **39**, 2522.
22 P. Pandey, O. K. Farha, A. M. Spokoyny, C. A. Mirkin, M. G. Kanatzidis, J. T. Hupp and S. T. Nguyen, *J. Mater. Chem.*, 2011, **21**, 1700.
23 O. Plietzsch, C. I. Schilling, T. Grab, S. L. Grage, A. S. Ulrich, A. Comotti, P. Sozzani, T. Muller and S. Bräse, *New J. Chem.*, 2011, **35**, 1577.
24 L.-H. Xie and M. P. Suh, *Chem.–Eur. J.*, 2013, **19**, 11590.
25 A. Phan, C. J. Doonan, F. J. Uribe-Romo, C. B. Knobler, M. O'Keeffe and O. M. Yaghi, *Acc. Chem. Res.*, 2010, **43**, 58.
26 K. Sumida, D. L. Rogow, J. A. Mason, T. M. McDonald, E. D. Bloch, Z. R. Herm, T. H. Bae and J. R. Long, *Chem. Rev.*, 2012, **112**, 724.
27 (*a*) P. Peng, F.-F. Li, F. Bowles, V. S. P. K. Neti, A. J. M. Magaña, M. Olmstead, A. Balch and L. Echegoyen, *Chem. Commun.*, 2013, **49**, 3209; (*b*) V. S. P. K. Neti, A. J. Metta-Magaña and L. Echegoyen, *J. Coord. Chem.*, 2013, **66**, 3193.
28 P. Peng, F.-F. Li, V. S. P. K. Neti, A. J. M. Magaña and L. Echegoyen, *Angew. Chem., Int. Ed.*, 2014, **53**, 160.
29 X. Feng, X. Ding and D. Jiang, *Chem. Soc. Rev.*, 2012, **41**, 6010.
30 J. W. Colson and W. R. Dichtel, *Nat. Chem.*, 2013, **5**, 453.
31 V. S. P. K. Neti, X. Wu, S. Deng and L. Echegoyen, *CrystEngComm*, 2013, **15**, 6892.
32 Z. Li, X. Feng, Y. Zou, Y. Zhang, H. Xia, X. Liu and Y. Mu, *Chem. Commun.*, 2014, **50**, 13825.
33 V. S. P. K. Neti, X. Wu, M. Hosseini, R. Bernal, S. Deng and L. Echegoyen, *CrystEngComm*, 2013, **15**, 7157.
34 T.-Y. Zhou, S.-Q. Xu, Q. Wen, Z.-F. Pang and X. Zhao, *J. Am. Chem. Soc.*, 2014, **136**, 15885.
35 M. Adinehnia, U. Mazur and K. W. Hipps, *Cryst. Growth Des.*, 2014, **14**, 6599–6606.
36 X.-H. Liu, Y.-P. Mo, J.-Y. Yue, Q.-N. Zheng, H.-J. Yan, D. Wang and L.-J. Wan, *Small*, 2014, **10**, 4934.
37 V. S. P. K. Neti, M. R. Cerón, A. Duarte-Ruiz, M. M. Olmstead, A. L. Balch and L. Echegoyen, *Chem. Commun.*, 2014, **50**, 10584.
38 A. V. Maffei, P. M. Budd and N. B. McKeown, *Langmuir*, 2006, **22**, 4225.
39 H. J. Mackintosh, P. M. Budd and N. B. McKeown, *J. Mater. Chem.*, 2008, **18**, 573.
40 M. Hashem, C. G. Bezzu, B. M. Kariuki and N. B. McKeown, *Polym. Chem.*, 2011, **2**, 2190.
41 F.-D. Cong, B. Ning, X.-G. Du, C.-Y. Ma, H.-F. Yu and B. Chen, *Dyes Pigm.*, 2005, **66**, 149.
42 G. K. B. Clentsmith, L. D. Field, B. A. Messerle, A. Shasha and P. Turner, *Tetrahedron Lett.*, 2009, **50**, 1469.
43 R. Dawson, D. J. Adams and A. I. Cooper, *Chem. Sci.*, 2011, **2**, 1173.
44 T. Islamoglu, M. G. Rabbani and H. M. El-Kaderi, *J. Mater. Chem. A*, 2013, **1**, 10259.

